Migration Letters

Volume: 21, No: S3 (2024), pp. 95-117

ISSN: 1741-8984 (Print) ISSN: 1741-8992 (Online)

www.migrationletters.com

A modified Indirect Matrix Converter with High Voltage Gain for Variable Speed Drive Application

Mohammed Ali Hussein Hweshim[1] , Zaid Hamodat[2] , Zaid Khalaf Mohammed Sadane[3]

ABSTRACT

For this paper, the literature review can be summarized as follows: QZSN was placed between the transformer phase in IMC and the rectifier phase. Inductor coils were used in the DC link and large capacitors, which increases the cost of the system in general.The non-continuous QZS-IMC technology was used to power the induction motor, and it is necessary to use an additional input filter to avoid harmonic frequencies from the current system. Closed input current control was used to reduce the frequency harmonics of the input current of the continuous intermittent control system to feed the R-L load. ZS/QZS-IMC was used with an R-L load, and the overwork ratio D was fixed at a certain value resulting in continuous boost, which is compatible with the constant voltage system . A method for controlling the maximum voltage of a DC motor closed circuit breaker based on QZS-IMC technology was used to correct the peak voltage value of the DC circuit breaker of an AC motor. As the continuous QZS-IMC was operated with the R-L load during the lowering and lifting modes, there was a control strategy to generate the time duty ratio of the exchange D. Continuous driving based on QZS-IMC technology was not used to drive a permanent magnet AC motor. In this paper, SVPWM was used to control the relays for the qzs-IMC continuous drive system of a carrier-controlled AC motor. A D-value control strategy has also been proposed based on the internal voltage and external voltage required for QZS-IMC to regulate the DC link voltage relative to the required speed and load. This strategy will contribute to reducing the current and voltage stresses of the power switches during voltage increase, by increasing the value of D in order to raise the internal voltage of the AC motor to the required level. Thus, the engine can be started at the required speed and load during various conditions .

Keywords: *Indirect matrix converter (IMC), Permeant magnet synchronous Motor (PMSM), Shoot through duty ratio (D), Space vector modulation (SVM),*

Quasi-z-source (QZS), Total harmonic distortion (THD).

1. INTRODUCTION

Variable speed AC motor drives have found extensive use in both industrial and household settings, including applications like textile mills, elevators, compressors, pumps, and washing machines [1]. AC-AC converter system is used to provide the variable speed AC drive[1]s With what is required amplitude of voltage and frequency depended on its control system and load [2]. The basic scheme of motor drive system is shown in figure (1), which illustrates that the AC motor is driven using AC-AC converter with rising AC voltage regulator of grid voltages.

[1]Electric and computer engineering Altinbas University Istanbul, Turkey
[2]Electric and computer engineering Altinbas University Istanbul, Turkey
[3]Zaid Khalaf Mohammed Sadane Northern Technical University

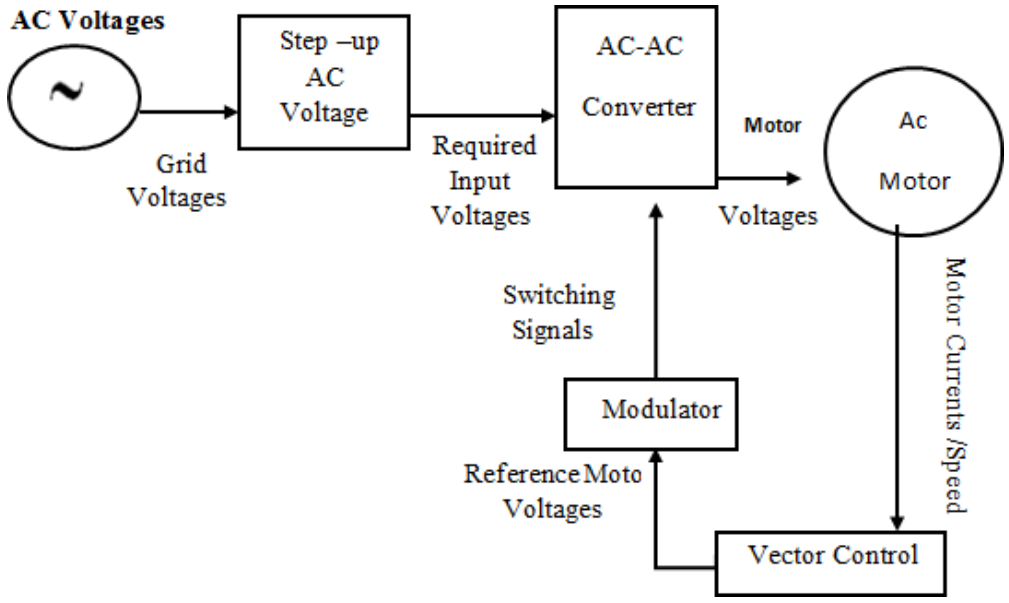

Figure 1: Basic scheme of motor drive system

AC-AC power conversion configurations are divided into two primary categories, depending on the presence or absence of passive energy storage components. The conventional AC-DC-AC converter comprises two stages: a group of unidirectional switches in the rectifier stage and another set of unidirectional switches in the inverter stage, with a DC-link capacitor positioned between the two stages. The utilization of a large DC-link capacitor in this setup can lead to increased costs, larger physical dimensions, higher losses, greater weight, and reduced reliability.In contrast, The matrix converter (MC) connects directly without the need for a capacitor to the DC connection, the AC source is connected to the load. It presents several advantages, such as a simplified and compact power circuit that eliminates the need for a DC-link capacitor, the ability to facilitate bidirectional power flow, generation of sinusoidal waveform input and output currents, and a unity power factor on the input side. Due to these beneficial features, the MC serves as a favorable alternative to the traditional AC-DC-AC converter [3].The MC can be further categorized into two types: the direct matrix converter (DMC) and the indirect matrix converter (IMC) [4]. The voltage and current are converted in one phase by DMC, which is referred to as direct power conversion. Conversely, the IMC carries out the conversion in two stages, known as indirect power conversion. Both the DMC and IMC deliver equivalent performance, and their circuit topologies share the same fundamental functionality. However, the DMC involves intricate commutation, In practical applications, any disparities in control performance between the DMC and IMC are entirely negligible [5]. The indirect matrix converter (IMC) has not garnered significant attention in industrial applications due to several issues. These problems include the limitation of the conventional IMC's voltage transfer ratio to 0.866 and the susceptibility to disturbances on either side of the IMC. This susceptibility arises because the power source connects directly to the load through an intermediate DC bus, causing disturbances on one side to affect the other [6]. Different topologies will form when the ZS/QZS network is connected to the IMC, and the resulting structure is called ZS/QZS-IMC. However, ZS/QZS-IMC has two different topologies depending on the QZS Network (QZSN) in the IMC and the location of the ZS Network (ZSN). The ZSN/QZSN can be placed between the rectifier stage and inverter stage of conventional IMC at the dc-link, the voltage gain becomes greater, but that it will cause an increase in size and weight of resulting converters since it needs large value of inductors and capacitors in comparison with the conventional IMC [7,8]. The other choice, where the ZSN/QZSN is integrated between power source and rectifier of IMC to avoid larger size and heavier weight of converter. IMC topology has the ability to achieve

high voltage gain and this is done using small ZSN/QZSN, this will be at high cost as it needs a large number of active switches. [9,10].

In this paper, the PMSM drived based on QZSIMC is fully explained by implementing simulations under voltage drop in the network, as well as speed and oscillating load conditions after explaining and presenting the operating principle of QZSIMC. Through the results, it was proven and demonstrated the possibility of QZSIMC and its ability to change the voltage gain depending on the required motor speed and the load situation.

2.1 . Z Source Indirect Matrix Converter Topology:

The ZSN system comprises of three inductors (L_a, L_b, L_c), three capacitors (C_a, C_b, C_c) and three bidirectional switches S_X (where x = a, b, c), as seen in figure (2). The control of these switches is achieved by the application of a single gate signal S_x as they exhibit identical switching characteristics. The implementation of the Zero Shot Neural (ZSN) model enables the ZS-IMC to operate in boost mode. However, the ZS-IMC topology has many disadvantages as: its voltage gain is constrained, it can only achieve gain of 1.15, The Z network causes phase shift, and it requires factors that increase the cost and size of the system, and this leads to a decrease in efficiency, as one of the most important factors is They are additional input filters to reduce harmonics in the input current due to intermittent grid current [11].

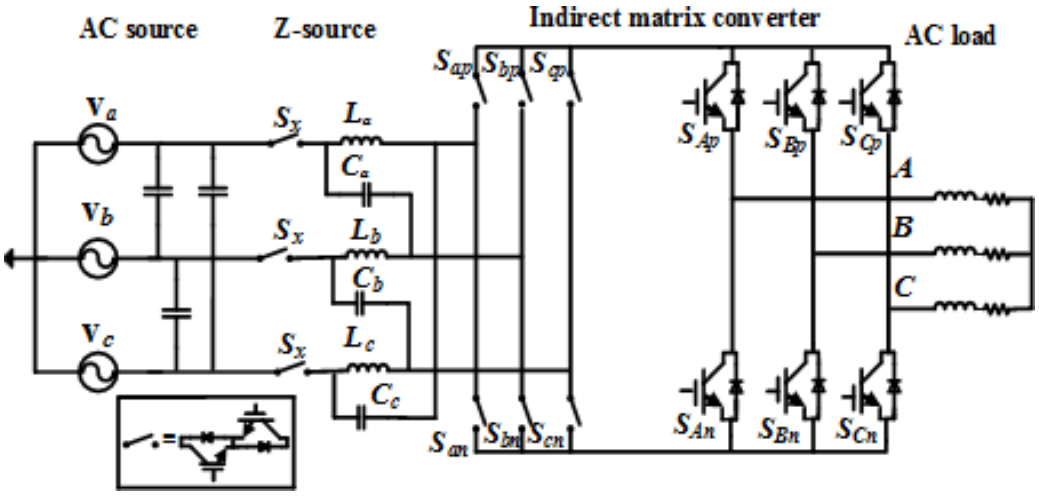

Figure 2 : ZS-IMC topology [12]

2.2 Operating Principle and Equivalent Circuits :

The diagram depicted in Figure (3) illustrates the configuration of the continuous QZS-IMC, which supplies power to a resistive-inductive (R-L) load during both the short-term (ST) and non-short-term (NST) states. Activating or deactivating the bidirectional switches of the QZS network (S_a, S_b, S_c) will result in the network operating in two distinct states. The initial state is denoted as non-short-term, as illustrated in figure (3-a). In the first case, the rectifier stage of the Integrated Motor Controller (IMC) operates conventionally, while the three switches of the Quadrature Zero Sequence Network (QZSN) are activated (S_X = 1). During the time period (1-D)T_s, As for the capacitors in the system, they are charged through inductors. It has been observed that the output voltage of the QZSN is equal to the sum of the voltages present across two capacitors [11].

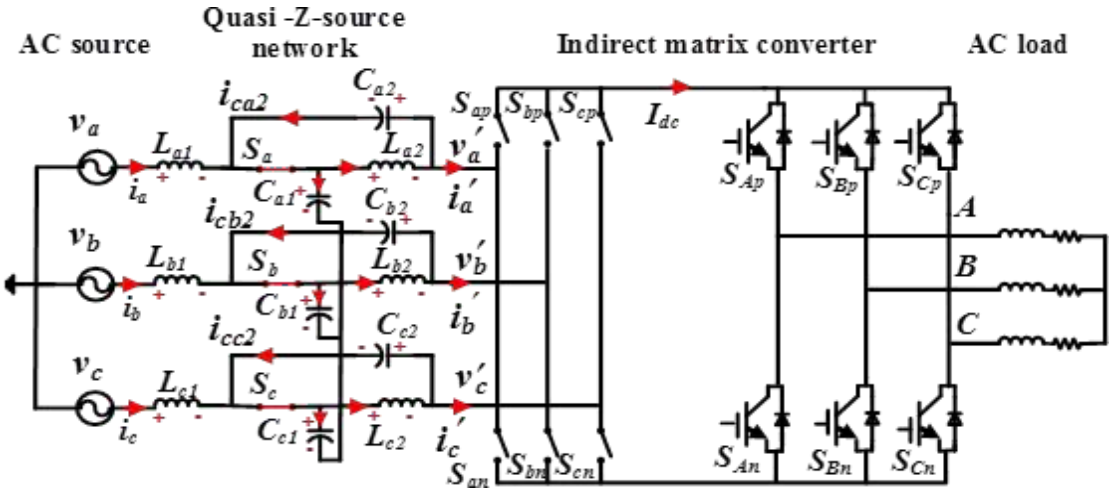

(a)

(b)

Due to $\mathbf{L_{a1}}$=$\mathbf{L_{a2}}$=$\mathbf{L_{b1}}$=$\mathbf{L_{a2}}$=$\mathbf{L_{c1}}$=$\mathbf{L_{c2}}$=L and $\mathbf{C_{a1}} = \mathbf{C_{a2}}$= $\mathbf{C_{b1}}$=$\mathbf{C_{b2}}$=$\mathbf{C_{c1}}$=$\mathbf{C_{c2}} = \mathbf{C}$

Figure 3 : (a) NST state of QZS-IMC and

(b) ST state of QZS-IMC [11].

from figure (3-a) assuming $\mathbf{R_L} = \mathbf{0}$, where $\mathbf{R_L}$is the stray resistance o

finductors, the following expressions can be obtained [12]:

$$\begin{bmatrix} v_{L_{a1}} \\ v_{L_{b1}} \\ v_{L_{c_1}} \end{bmatrix} = \begin{bmatrix} v_a \\ v_b \\ v_c \end{bmatrix} - \begin{bmatrix} v_{c_{a1}} \\ v_{c_{b1}} \\ v_{c_{c_1}} \end{bmatrix} \quad (1)$$

$$\begin{bmatrix} v_{La1} \\ v_{L_{b1}} \\ v_{L_{c_1}} \end{bmatrix} = \begin{bmatrix} v_a \\ v_b \\ v_c \end{bmatrix} + \begin{bmatrix} v_{c_{a2}} \\ v_{c_{b2}} \\ v_{c_{c_2}} \end{bmatrix} - \begin{bmatrix} v_a^{'} \\ v_b^{'} \\ v_c \end{bmatrix} \quad (2) \quad .$$

The QZSN inductor-L_2 voltages $v_{L_2} = [v_{L_{a2}} \quad v_{L_{b2}} \quad v_{L_{c_2}}]^T$ are:

$$\begin{bmatrix} v_{L_{a2}} \\ v_{L_{b2}} \\ v_{L_{c_2}} \end{bmatrix} = - \begin{bmatrix} v_{c_{a2}} \\ v_{c_{b2}} \\ v_{c_{c_2}} \end{bmatrix} \quad (3).$$

The QZSN capacitor-C_1 currents $i_{C_1} = [i_{C_{a1}} \quad i_{C_{b1}} \quad i_{C_{c1}}]^T$ are:

$$\begin{bmatrix} i_{C_{a1}} \\ i_{C_{b1}} \\ i_{C_{c1}} \end{bmatrix} = \begin{bmatrix} i_{L_{a1}} \\ i_{L_{b1}} \\ i_{L_{c1}} \end{bmatrix} - \begin{bmatrix} i_a^{'} \\ i_b^{'} \\ i_c \end{bmatrix} \quad (4)$$

The QZSN capacitor-C_2 currents $i_{C_2} = [i_{C_{a2}} \quad i_{C_{b2}} \quad i_{C_{c2}}]^T$ are:

$$\begin{bmatrix} i_{C_{a2}} \\ i_{C_{b2}} \\ i_{C_{c2}} \end{bmatrix} = \begin{bmatrix} i_{L_{a2}} \\ i_{L_{b2}} \\ i_{L_{c2}} \end{bmatrix} - \begin{bmatrix} i'_a \\ i'_b \\ i'_c \end{bmatrix} \quad (5)$$

where : $[i'_a \; i'_b \; i'_c]^T$ are the output currents of QZSN. In contrast, in the ST state, the switches of QZSN are deactivated ($S_x = 0$) depicted in figure (3-b). The input side of the rectifier stage is effectively connected in a short-circuit configuration, The QZSN inductors are allowed to charge in each phase during one switching cycle. The shoot-through duty cycle, denoted as D, is defined as the ratio of the time interval of the ST state, T_0, to the total switching period, D= T_0/T_s.The expressions presented in figure (7-b) [12] can be derived [12].

The voltages between the QZSN inductoL_1 and inductor-L_2 are as follows:

$$\begin{bmatrix} v_{L_{a1}} \\ v_{L_{b1}} \\ v_{L_{c_1}} \end{bmatrix} = \begin{bmatrix} v_a \\ v_b \\ v_c \end{bmatrix} + \begin{bmatrix} v_{c_{a2}} \\ v_{c_{b2}} \\ v_{c_{c_2}} \end{bmatrix} \quad (6)$$

$$\begin{bmatrix} v_{c_{a1}} \\ v_{c_{b1}} \\ v_{c_{c_1}} \end{bmatrix} = \begin{bmatrix} v_{L_{a2}} \\ v_{L_{b2}} \\ v_{L_{c_2}} \end{bmatrix} \quad (7)$$

The QZSN capacitor - C_1 currents and capacitor - C_2 currents are:

$$\begin{bmatrix} i_{C_{a1}} \\ i_{C_{b1}} \\ i_{C_{c1}} \end{bmatrix} = - \begin{bmatrix} i_{L_{a2}} \\ i_{L_{b2}} \\ i_{L_{c2}} \end{bmatrix} \quad (8)$$

$$\begin{bmatrix} i_{L_{a1}} \\ i_{L_{b1}} \\ i_{L_{c1}} \end{bmatrix} = - \begin{bmatrix} i_{C_{a2}} \\ i_{C_{b2}} \\ i_{C_{c2}} \end{bmatrix} \quad (9)$$

$$\begin{bmatrix} v_{L_{a1}} \\ v_{L_{b1}} \\ v_{L_{c_1}} \end{bmatrix} = D\left(\begin{bmatrix} v_a \\ v_b \\ v_c \end{bmatrix} + \begin{bmatrix} v_{c_{a2}} \\ v_{c_{b2}} \\ v_{c_{c_2}} \end{bmatrix}\right) + (1-D)\left(\begin{bmatrix} v_a \\ v_b \\ v_c \end{bmatrix} - \begin{bmatrix} v_{c_{a1}} \\ v_{c_{b1}} \\ v_{c_{c_1}} \end{bmatrix}\right) = 0 \quad (10)$$

$$\begin{bmatrix} v_{L_{a2}} \\ v_{L_{b2}} \\ v_{L_{c_2}} \end{bmatrix} = D \begin{bmatrix} v_{c_{a1}} \\ v_{c_{b1}} \\ v_{c_{c_1}} \end{bmatrix} + (1-D)\left(-\begin{bmatrix} v_{c_{a2}} \\ v_{c_{b2}} \\ v_{c_{c_2}} \end{bmatrix}\right) = 0 \quad (11)$$

$$\begin{bmatrix} i_{C_{a1}} \\ i_{C_{b1}} \\ i_{C_{c1}} \end{bmatrix} = D\left(-\begin{bmatrix} i_{L_{a2}} \\ i_{L_{b2}} \\ i_{L_{c2}} \end{bmatrix}\right) + (1-D)\left(\begin{bmatrix} i_{L_{a1}} \\ i_{L_{b1}} \\ i_{L_{c1}} \end{bmatrix} - \begin{bmatrix} i'_a \\ i'_b \\ i'_c \end{bmatrix}\right) = 0 \quad (12)$$

$$\begin{bmatrix} i_{C_{a2}} \\ i_{C_{b2}} \\ i_{C_{c2}} \end{bmatrix} = D\left(-\begin{bmatrix} i_{L_{a1}} \\ i_{L_{b1}} \\ i_{L_{c1}} \end{bmatrix}\right) + (1-D)\left(\begin{bmatrix} i_{L_{a2}} \\ i_{L_{b2}} \\ i_{L_{c2}} \end{bmatrix} - \begin{bmatrix} i'_a \\ i'_b \\ i'_c \end{bmatrix}\right) = \mathbf{0} \quad (13)$$

The capacitor voltages and inductor currents of the QZSN system can be determined by referring to equations (10) through (13):

$$\begin{bmatrix} v_{c_{a1}} \\ v_{c_{b1}} \\ v_{c_{c_1}} \end{bmatrix} = \frac{(1-D)}{(1-2D)} \begin{bmatrix} v_a \\ v_b \\ v_c \end{bmatrix} \quad (14)$$

$$\begin{bmatrix} v_{c_{a2}} \\ v_{c_{b2}} \\ v_{c_{c_2}} \end{bmatrix} = \frac{D}{(1-2D)} \begin{bmatrix} v_a \\ v_b \\ v_c \end{bmatrix} \quad (15)$$

$$\begin{bmatrix} i_{L_{a2}} \\ i_{L_{b2}} \\ i_{L_{c2}} \end{bmatrix} = \begin{bmatrix} i_a \\ i_b \\ i_c \end{bmatrix} \quad (16)$$

$$\begin{bmatrix} i_{L_{a1}} \\ i_{L_{b1}} \\ i_{L_{c1}} \end{bmatrix}$$

According to equations (14) through (16):

$$\begin{bmatrix} i'_a \\ i'_b \\ i'_c \end{bmatrix} = \frac{(1-2D)}{(1-D)} \begin{bmatrix} i_a \\ i_b \\ i_c \end{bmatrix} \quad (17)$$

$$\begin{bmatrix} v'_a \\ v'_b \\ v'_c \end{bmatrix} = \frac{1}{1-2D} \begin{bmatrix} v_a \\ v_b \\ v_c \end{bmatrix} \quad (18)$$

As for β, which is called the voltage boost factor , it can be represented mathematically as follows: $\beta = \frac{v_i^F}{v_i} = \frac{1}{1-2D}$ (D < 0.5) (19)

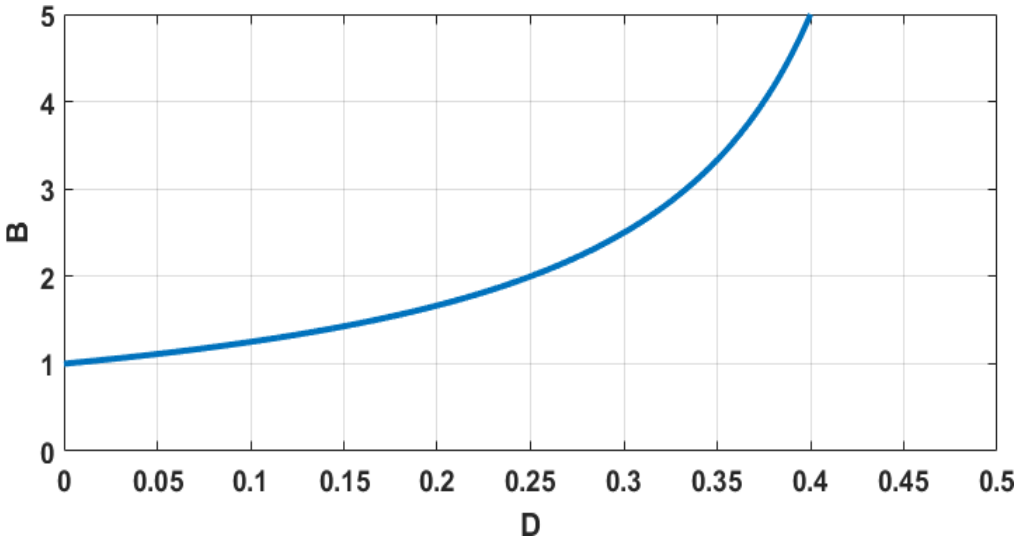

Figure 4 : Voltage boost factor versus D [12].

It is obvious from the figure (4), that the value of boost factor reaches 5 at D = 0.4, which means that five times voltage amplitude is obtainable in comparison with the source voltage.

The average dc-link voltage of the QZS-IMC is obtained as:The input power after the QZSN is equal to the output power of the front -end rectifier of the IMC [13].

$P_{dc} = P_{in}$ (20)

$$\bar{V}_{dc}\bar{I}_{dc} = 3V'_{i\,(rms)}I'_{i\,(rms)}\cos(\theta_{QZS}) \quad (21)$$

$$\bar{V}_{dc}\,\bar{I}_{dc} = \frac{3}{2}V'_i\,I'_i\cos(\theta_{QZS}) \quad (22)$$

$$m_i = \frac{I_i^F}{\bar{I}_{dc}} \quad (23)$$

$$\bar{V}_{dc} = \frac{3}{2}V'_i\,m_i\cos(\theta_{QZS}) \quad (24)$$

$$\bar{V}_{dc} = \frac{3}{2}V_i\,\beta\,m_i\cos(\theta_{QZS}) \quad (25)$$

where: $\bar{I}_{dc}$ represents value average of dc-link current.

From equations ($m_0 = \frac{\sqrt{3}V_o}{\bar{V}_{dc}}$) and equations (25) with $\cos(\theta_{QZS})$=1, the voltage gain (G) of the continuous QZS-IMC is obtained as [15]:

$$G = \frac{V_o}{V_i} = \frac{3/2\,\bar{V}_{dc}m_0\,\beta\,m_i}{\sqrt{3}\,\bar{V}_{dc}} = \frac{\sqrt{3}\,m_0\,m_i}{2\;1-2D} = \frac{\sqrt{3}}{2}\beta\,m \quad (26)$$

where $m = m_i m_0$, D = $1 - m_i$,for simplification m_0 =1.

$$= \frac{0.866\, m_i}{2m_i - 1} \qquad (27) \qquad G = \frac{0.866\, m_i}{1-2D}$$

5. Parameters Design of Quasi Z Source Network:

The ripples of capacitor voltage and inductor current for the continuous QZS- IMC can be calculated as follows [10]:
From the NST and ST states, the inductor current ripple (Δl_{L_1}) and capacitor voltage ripple (Δv_{C_1}) can be expressed as [13]:

$$\Delta l_{L_1} = \frac{v_{L_1}(1-D)}{f_s L_1} \qquad (28)$$

$$\Delta v_{C_1} = \frac{i_{C_1} D}{f_s C_1} \qquad (29)$$

$$\Delta l_{L_1} = \frac{|v_x - v_{C_1}|(1-D)}{f_s L} = \frac{V_i\, D(1-D)}{(1-2D) f_s L} \qquad (30)$$

$$\frac{\Delta i_{L1}}{K_L} = \frac{D(1-D)}{(1-2D)} \qquad (31)$$

During ST state, the capacitor- C_1current and inductor-L_2 current are equal.

$$\Delta v_{C_1} = \frac{i_{L_2} D}{f_s C_1} = \frac{i_x D}{f_s C_1} = \frac{P_{in} D}{3 V_x f_s C_1 cos(\theta_i)} = \frac{P_{in} D}{3 V_i f_s C_1 cos(\theta_i)} \qquad (32)$$

$$\frac{\Delta v_{C_1}}{K_C} = D \qquad (33)$$, where : x = (a, b, c), and the coefficients k_L and k_C are:

$$K_L = \frac{V_i}{f_s L} \text{ , } K_C = \frac{P_{in}}{3 V_i f_s C_1 cos(\theta_i)} \qquad (34)$$

where: P_{in} and f_s are the input power and switching frequency, respectively.

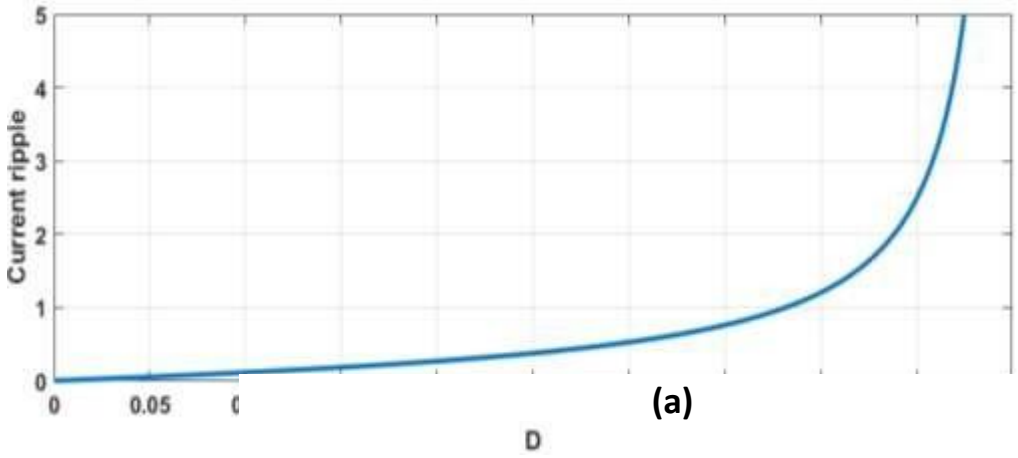

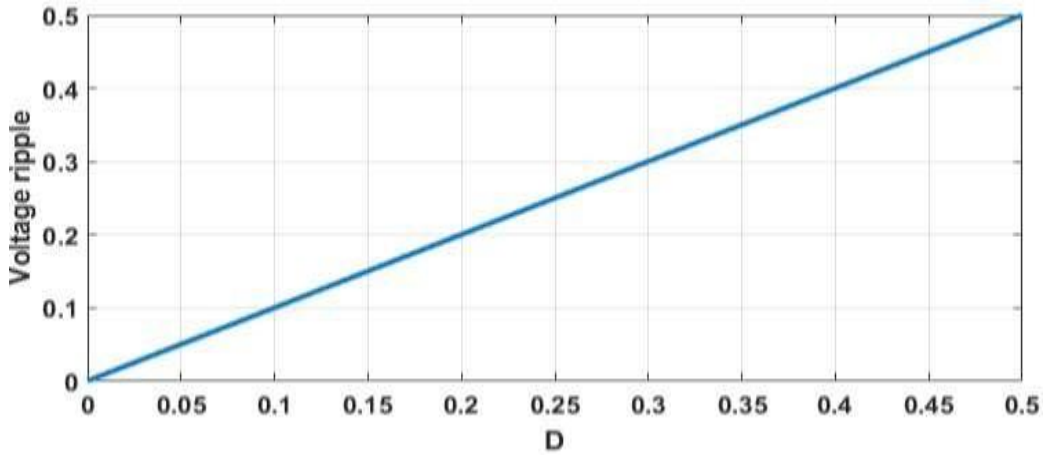

(b)

Figure 5 : (a) Current ripple versus D (b) Voltage ripple versus D

It can be seen from figure (5-a), that current ripple for continuous QZS-IMC increases in nonlinear manner when the D increases, while and voltage ripple increase linearly when the shoot-through duty ratio increases, as shown in figure (5-b) when all parameters as; the input power and voltage, capacitance, and inductance are constant.Then, the QZSN inductance and capacitance are derived as follows [14]:

$\Delta i_L = k_1 I_{rated}$ (35)

From equation (30)

$L = \frac{\frac{V_i D(1-D)}{(1-2D)}}{f_s k_1 I_{rated}}$, $L \geq \frac{V_i D(1-D)}{f_s k_1 I_{rated}\,(1-2D)}$ (36)

$\Delta v_C = k_2 V_{C_{rated}}$ (47)

From equation (32) $C = \frac{I_{rated} D}{f_s k_2 V_i (\frac{1-D}{1-2D})}$, $C \geq \frac{I_{rated}(1-2D)D}{f_s k_2 V_i (1-D)}$ (37)

where: Δi_L and Δv_C are peak values of ripples for current and voltage, respectively.

The cut-off frequency ω_n from the small-signal analysis are [10]:

$\omega_n = \frac{1-2D}{\sqrt{Lc}} \leq \frac{2\pi f_s}{10}$ (38)

7. CONTROL STRATEGY OF D :

According to this equation ($G = \frac{0.866\, m_i}{1-2D} = \frac{0.866\, mi}{2m_i - 1}$) and taking $m_i = 1 - D$, the voltage transfer ratio of QZS-IMC is:

$= 0.866 \frac{(1-D)}{1-2D}$ (39) , $\frac{V_O}{V_i}$

Then, the value of D is established as:

$D = \frac{V_0 - 0.866\, V_i}{2\, V_0 - 0.866\, V_i}$ (40) ,

control algorithm for D is as shown Figure(6) :

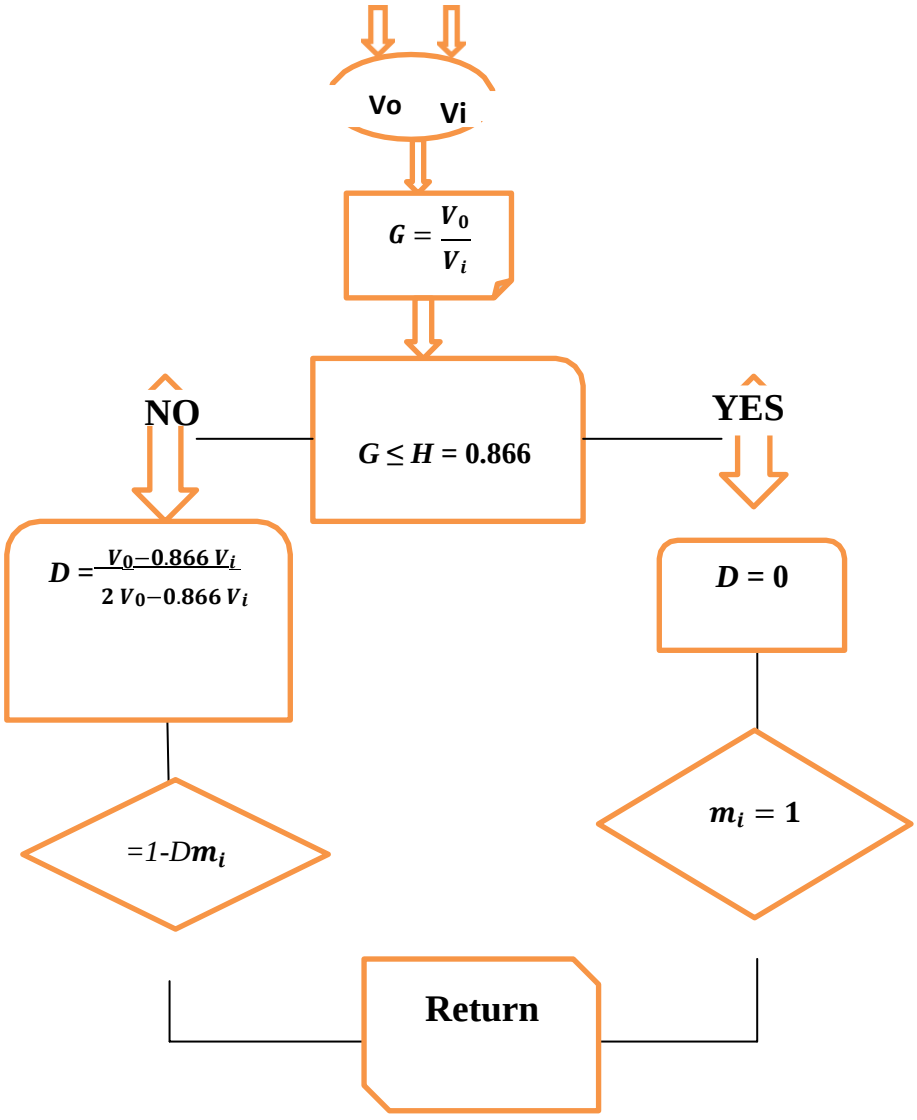

Figure 6 : Flowchart for optimal operation control of D

8. Vector Control of PMSM:

This means that it is a high-performance control technology, as its control method is equal to the speed control method for direct current devices. [15]. Through this equation ($\omega_r = \int \left(\frac{T_e - T_L - B\,\omega_r}{J}\right) \cdot dt$), it is noted that by controlling the resulting torque, we can control the speed of the engine. As for the type of PMSM that is mounted on the surface, It was noted that ($L_q = L_d$) ,then from equation ($T_e = \frac{3}{2}\frac{p}{2}(\lambda_d i_q - \lambda_q i_d)$) the generated torque is expressed as:

$$T_e = \frac{3}{2}\frac{p}{2}(\lambda_m i_q) \quad (50)$$

the Park-Clarke transformation is able to derive id and iq.This transformation accounts for the flux generation and torque components of the stator current.This information is sourced from reference [16].

$$\begin{bmatrix} i_d \\ i_q \end{bmatrix} = \frac{2}{3}\begin{bmatrix} \cos\theta & \cos(\theta-\alpha) & \cos(\theta-2\alpha) \\ -\sin\theta & -\sin(\theta-\alpha) & -\sin(\theta-2\alpha) \end{bmatrix} \begin{bmatrix} i_A \\ i_B \\ i_C \end{bmatrix} \quad (51)$$

In equations (51) and (52), $\omega_e L_q\, i_q$ and $-\omega_e(L_d i_d + \lambda_m)$ are coupling terms. When the engine speed is high, we cannot neglect its effect in figure (7) .

$$v_d^{**} = -\omega_e L_q\, i_q \quad (51)$$

$$v_q^{**} = \omega_e\,(L_d i_d + \lambda_m) \quad (52)$$

The main objective of decoupling control is to achieve repaid dynamic response, as well as to get good steady-state performance and to control the i_d and i_q separately [17].

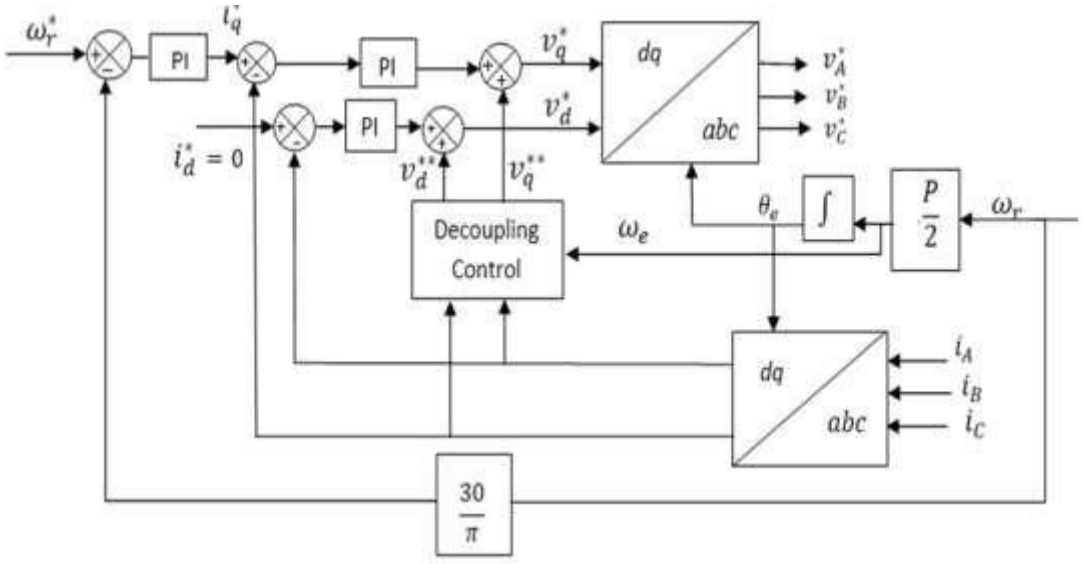

Figure 7 : Block diagram of proposed vector control. [17]

6. Proposed QZS -IMC based PMSM Drive:

This thesis utilizes the continuous Quasi-Z-Source Network (QZSN) as a means to enhance the dc-link voltage, thereby establishing a connection between the three-phase supply voltage and the Integrated Motor Controller (IMC), as illustrated in figure (8). The IMC topology of continuous QZS-IMC has two stages: the rectifier stage and the inverter stage. The primary function of the rectifier stage is to maintain the highest positive voltage inside the direct current (dc) link, while also achieving sinusoidal grid currents on the input side. The inverter stage control is responsible for generating the output voltages of QZS-IMC with adjustable frequency and amplitude. The rectifier stage of the IMC use SVPWM to modulate the input current, while the inverter stage utilizes SVPWM to modulate the output voltage, as depicted in Figure (8) [10]

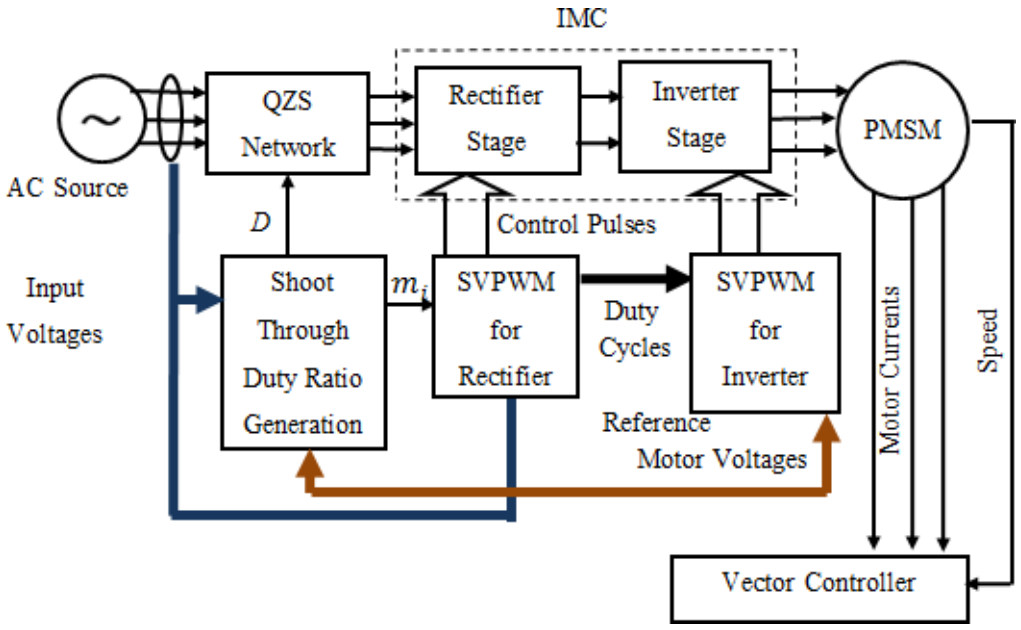

Figure 8 : Block diagram of Proposed QZS-IMC fed PMSM drive

9. SIMULATION RESULTS:

For all conditions, the simulation is performed for a switching frequency of 10 kHz and the simulation results are obtained using MATLAB/ Simulink 2018b. The contents of the system are displayed, the values taken are displayed, and then the results are obtained.

Divided into three cases according to the speeds taken:

Table 1: PMSM Drive Specifications

Parameters	**Value**
Rated power	1.1 kW
Rated speed	3000 rpm
DC voltage	300 V
Stator q inductance, L_q	0.0085 H
Stator d inductance, L_d	0.0085 H
Stator resistance, R_s	2.875 Ω
Moment of inertia , J	0.0008 $Kg.m^2$
Friction factor, B	0.001 N.m.s
Flux linkage, λ_m	0.175 Wb
Number of poles , p	4
Rated torque	3 N.m

Table 2: parameters of QZSN

Parameters	**Value**
Three-phase voltage source	110V/50Hz
Inductance	5mH
Capacitance $of\ QZSN\ C_1$	10 µF
Capacitance $of\ QZSN\ C_2$	30 µF
Capacitor voltage ripple ratio (k_2)	13%
Inductor current ripple ratio (k_1)	5%
Switching frequency	10 kHz

Firstly, In order to study the transient and steady-state behavior of the drive system, simulations were performed for variable reference speeds of 750, 1500, 2250 and 3000 rpm at rated load with an input stage voltage amplitude of 110 V and a frequency of 50 Hz as shown in Figure (9), the simulation time is 4 seconds. The initial conditions for this

simulation are as follows: the estimated engine load is 3 Nm, and the initial response speed is between 0 and 750 rpm. After this process, the speed increases to 1500 rpm in one second and then to 2250 rpm in one second. After 2 seconds, the speed is finally set to 3000 rpm (rated speed) over a period of 3 seconds.

Table 3: Parameters of QZS-IMC with RL Load

Parameters	**Value**
Power rating	1.5 kW
Amplitude of input voltage	50 V
Capacitance of QZS network	300 μF
Inductance of QZS network	2 mH
Switching frequency, f_s	10 kHz
Input voltage frequency	50 Hz
Output voltage frequency	30 Hz
Load resistance,R_L	5 Ω
Load inductance,L_L	3 mH

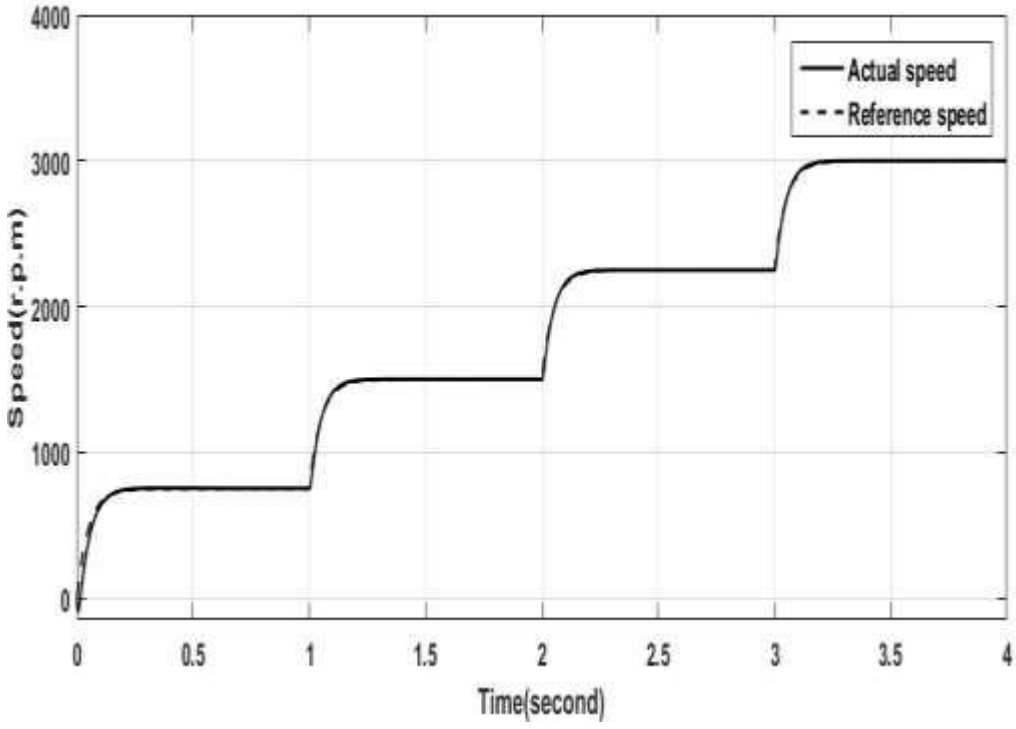

Figure 9 : (The speed response of QZS-IMC based motor driveat variable speed)

Figure (10. a) and figure (10. b) show the response of torque and d-q currents, respectively

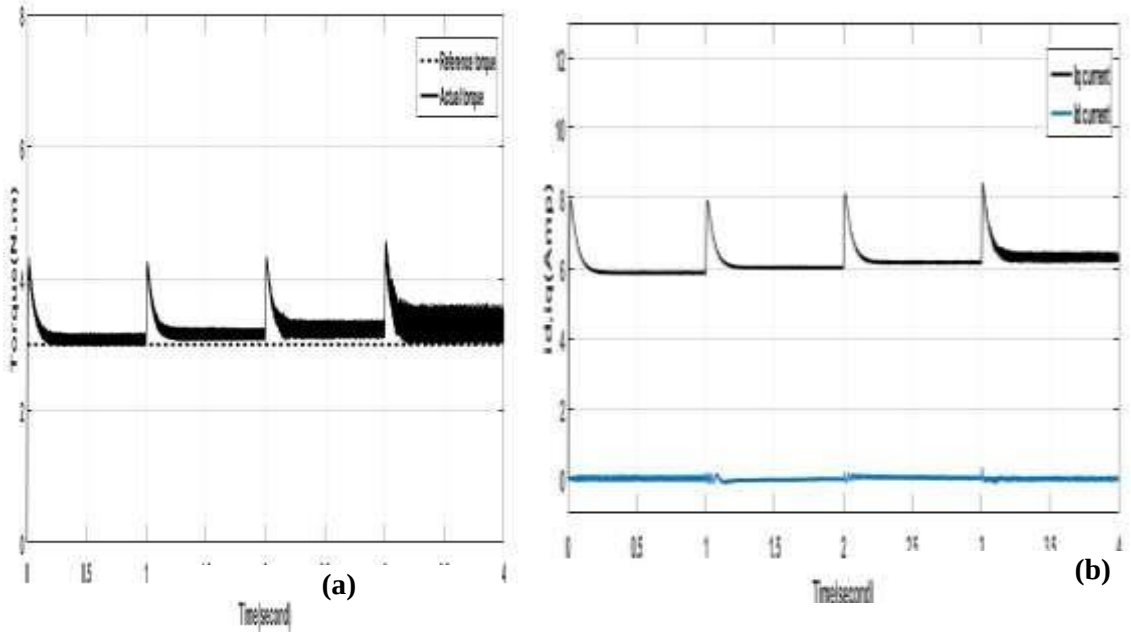

Figure 10: (a) The torque response of QZS-IMC, (b) The d-q currents of QZS-IMC

The phase -a It shows us the source of current and voltage The THDs of the phase-a source current are 3.87% , 2.37% , 2.83% and 4.65% with input power factor of 0.9876, 0.998, 0.9982 and 0.9984 for speeds 750, 1500, 2250 and 3000 rpm, respectively and as shown in Figure (11):

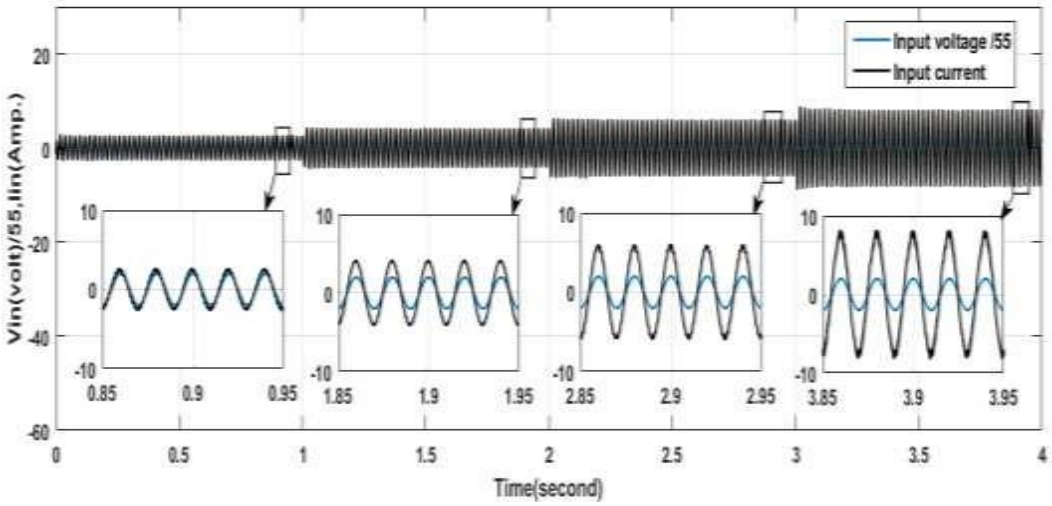

Figure11 : The phase-a source current and voltage waveforms of the QZS-IMC based motor drive at variable speed

The THD ratios for the stator current waveform are as follows: 1.68%, 1.65%, 1.99% and 3.77% for speeds of 750, 1500, 2250 and 3000 rpm, respectively and as shown in Figure (12):

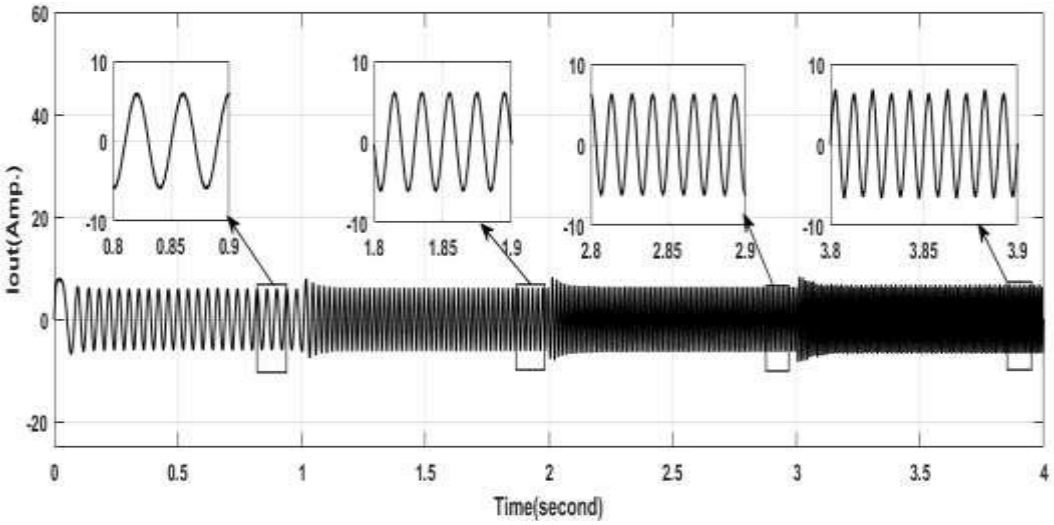

Figure 12: The phase -A stator current waveform of QZS-IMC based motor drive at variable

It is shown in the figure (13) The value of D equal zero for first 2 seconds of the period because of the required voltage gain of QZS-IMC is less than 0.866, so Since increasing the voltage is not necessary, QZSN would serve as a second-tier candidate. The value of D will increase from 0 to 0.075 and from 0.075 to 0.225 after 2 and 3 seconds,respectively, According to the optimal operation control flow chart of D in Figure (14), the required voltage gain of QZS-IMC is greater than 0.866.

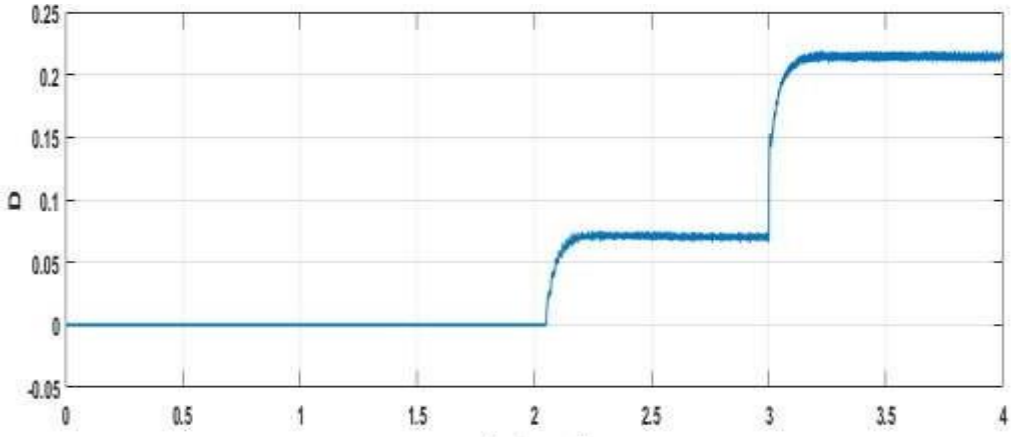

Figure 13 : Shoot -through duty ratio response of QZS-IMC based motor drive system at variable speed

As a result, to operate the motor at the required speed and load, it will result in an enhancement of the DC link voltage and the output voltage, as shown in the figure (14. a) and figure (14. b), respectively

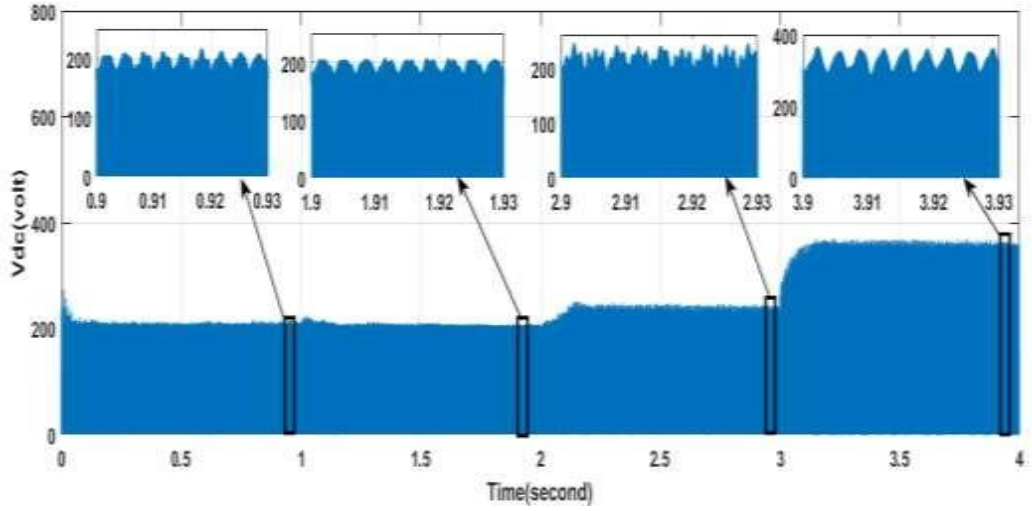

(a)

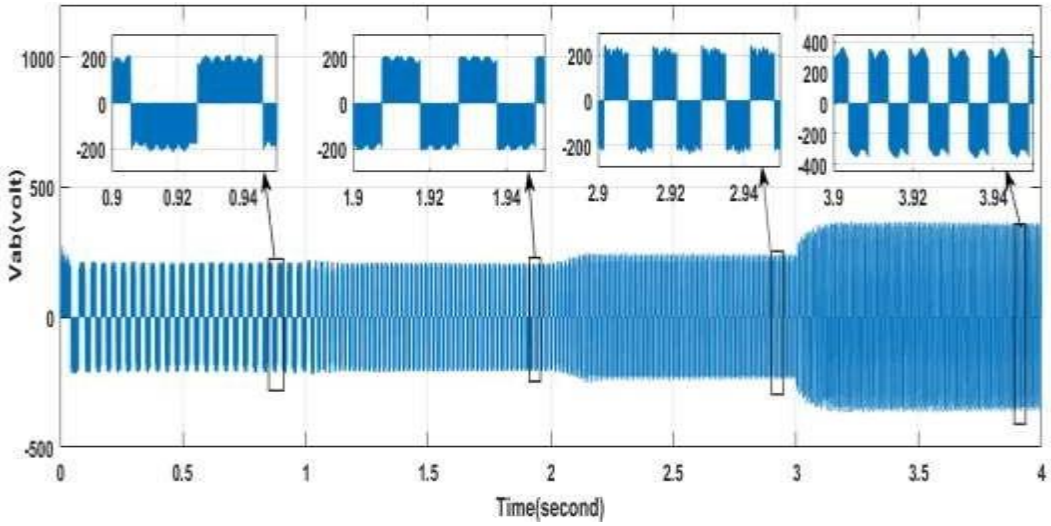

(b)

Figure 14 :(a) Waveform of dc-link voltage and (b) Waveform of output voltage of QZS-IMC based motor drive at variable speed

Secondly, the drive system is tested with input phase voltage amplitude of 110 V and frequency of 50 Hz for different reference speeds (750, 1500, 2250 and 3000 rpm) under

variable load of 1, 2 and 3 Nm for each reference speed in order to prove the proposed operation strategy of QZS-IMC

for PMSM drive system under step change of load torque for each speed.At motor speed of 750 rpm, the system is run with variable load, the speed response is shown in figure (15), it is clear that the motor speed follows the reference and returns to its reference after a step change in load happen.

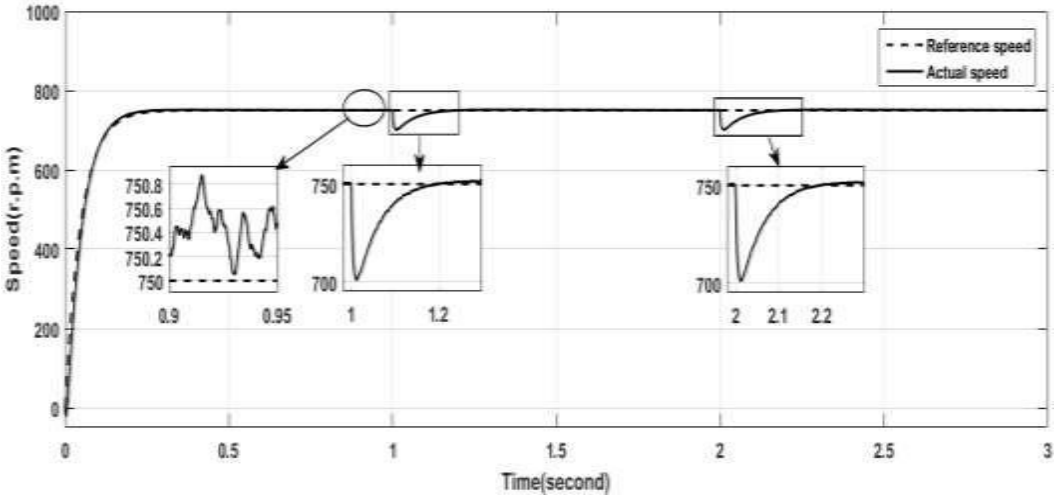

Figure 15 : The speed response of QZS-IMC based motor drive at 750 rpm and variable load

The load is increased from 1 to 2 and from 2 to 3 Nm at times of 1 and 2 second, respectively, as shown in figure (16). The speed response shows disturbance with downshoot of 6.666% and very small overshoot, and returns to actual value after 0.5 second for both load step changes, the peak to peak steady state ripple in speed is calculated as: (750.97 – 750.02) / 750.45)*100 % = 0.126% for load 1 Nm, and it is equal to 0.106% and 0.0932% for loads 2 and 3 Nm at steady state, respectively.

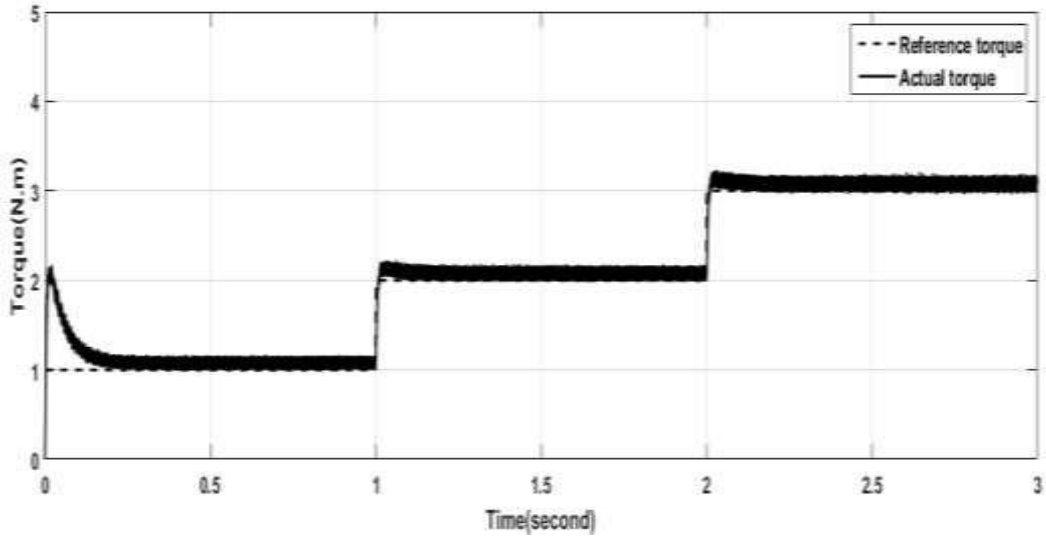

Figure 16 : The torque response and

The d-q currents response demonstrate that the PI controller is able to keep the value of i_d at zero, while the i increases with load increasing.
Figure (17) shows the waveforms of the source current and input voltage. the source current is sinusoidal waveform with small distortion, and the source current is approximately in phase with input voltage. The THDs of the source current are 5.44%, 4.23% and 3.87% with input power factor of 0.91, 0.9759 and 0.9876 for loads of 1, 2 and 3 Nm , respectively.

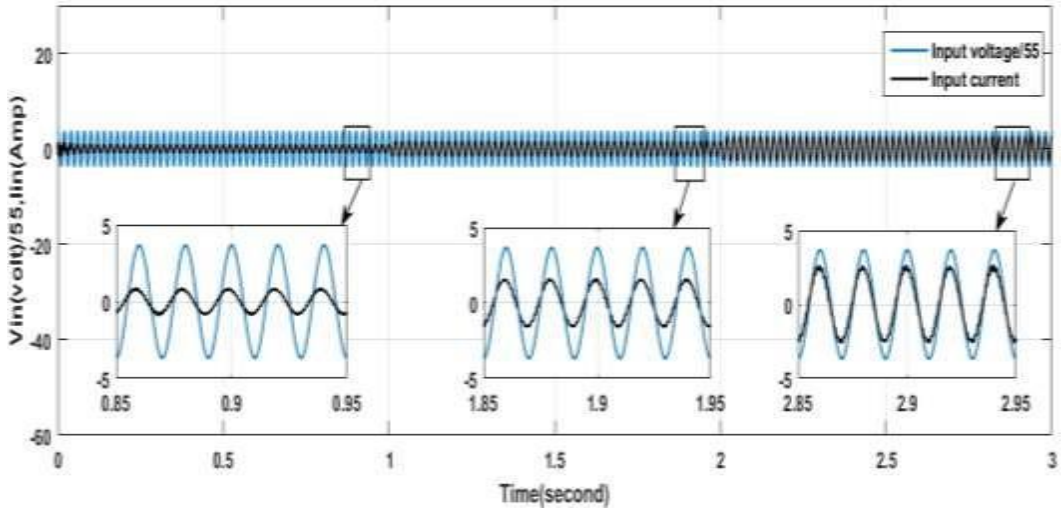

Figure 17 : The phase-a source current and voltage waveforms of QZS-IMC based motor drive at 750 rpm and variable load

As shown in Figure (18), the stator current waveform has a THD of 3.31%, 2.03%, and 1.68% for loads of 1, 2, and 3 Nm, respectively.

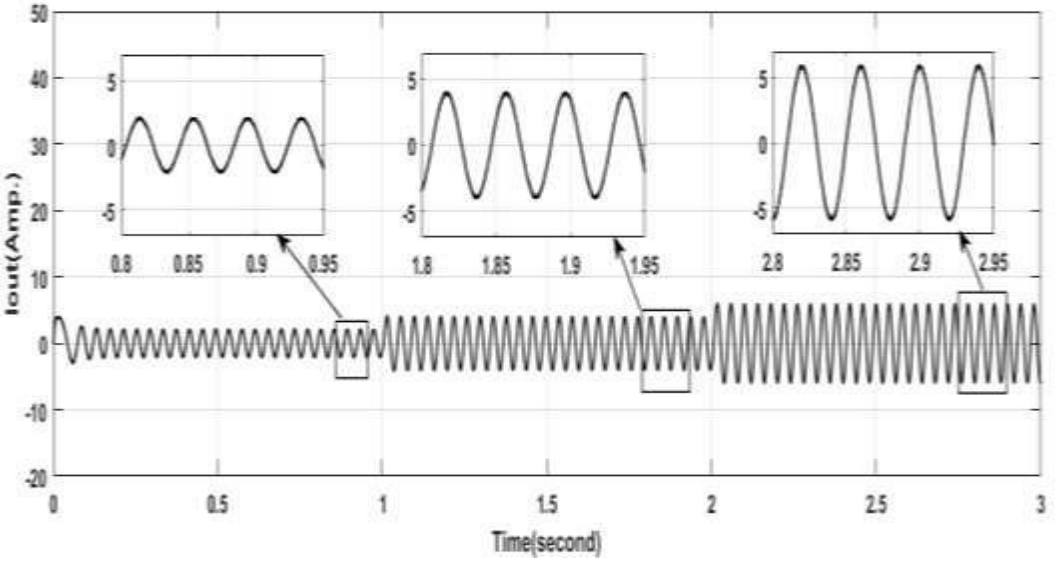

Figure 18 : The phase -A stator current waveform of QZS-IMC based motor drive at 750 rpm and variable load

With the motor speed of 750 rpm, the output frequency is 25 Hz, and the required output voltage gain of QZS-IMC is less than 0.866, so there is no need to boost dc-link voltage, as

shown in figure (19). Thus, the QZS network will only work as a filter, D=0, and m_i =1, where the QZS-IMC is running as a conventional IMC with no shoot-through.

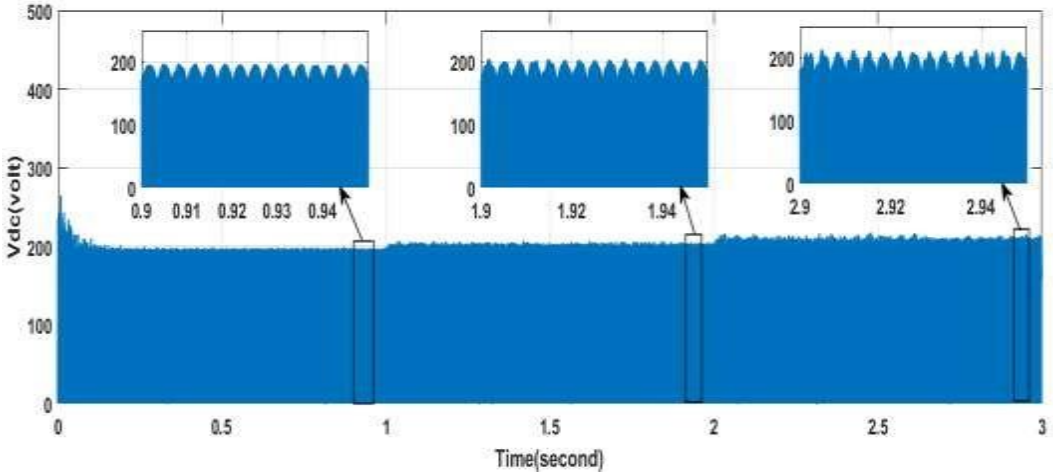

Figure 19: DC-link voltage waveform of QZS-IMC based motor drive at 750 rpm and variable load

The system is tested with speed of 1500 rpm under variable load, the speed response is shown in figure (20), it is clear that the motor speed follows the reference with a good response.

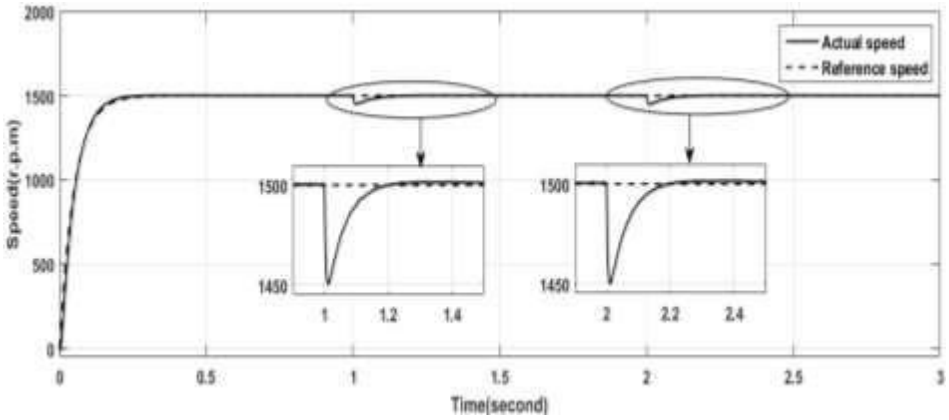

Figure 20 : The speed response of QZS-IMC based motor drive at 1500 rpm and variable

The load as shown in figure (21. a) is increased from 1 to 2 and from 2 to 3 Nm at times of 1and 2 second, respectively, the speed response shows disturbance with downshoot of 3.33% and very small overshoot, and returns to actual value after 0.46 second for both step changes of load, the peak to peak steady state ripple in speed is seen to be 0.0633%, 0.0526% and 0.0533% for loads 1, 2 and 3 Nm, respectively. The response of the d-q currents is shown in figure (21. b).

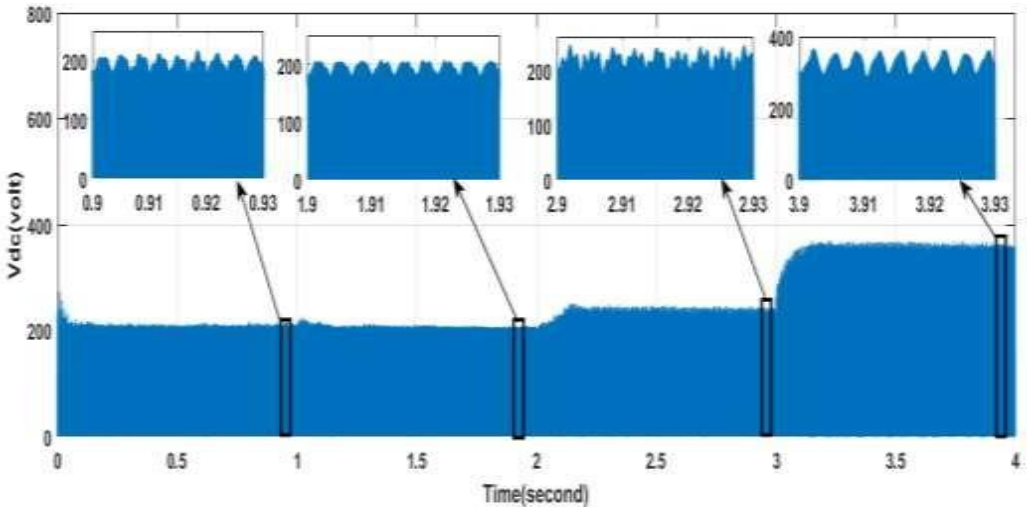

(a)

Figure 21: (a) Waveform of dc-link voltage and (b) Waveform of output voltage of QZS-IMC based motor drive at variable speed

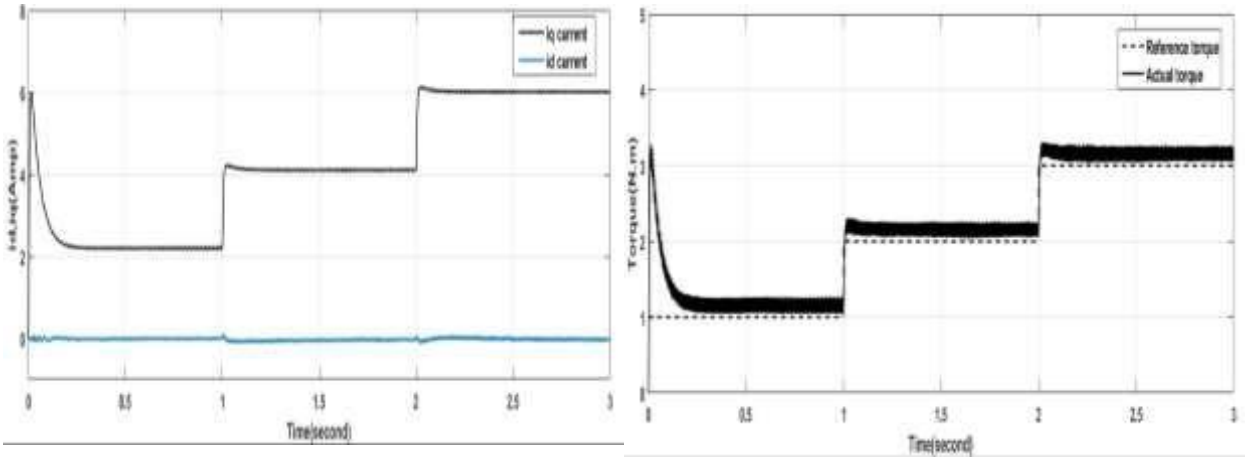

Figure 21 : (a) The torque response and (b) The d-q currents of QZS- IMC based motor drive at 1500

(a) **(b)**

Third: The system operates in the third state with a rated load at 3000 rpm. then voltage sag of 20% occurs at time 1 until 2 second. The amplitude of input phase voltage is decreased from 110 V to 88 V as shown in the figure (22. a). It is seen from figure (22. b) that required voltage gain for motor at speed of 3000 rpm is 1.43 during voltage sag. Hence, the value of D is increased to 0.288,

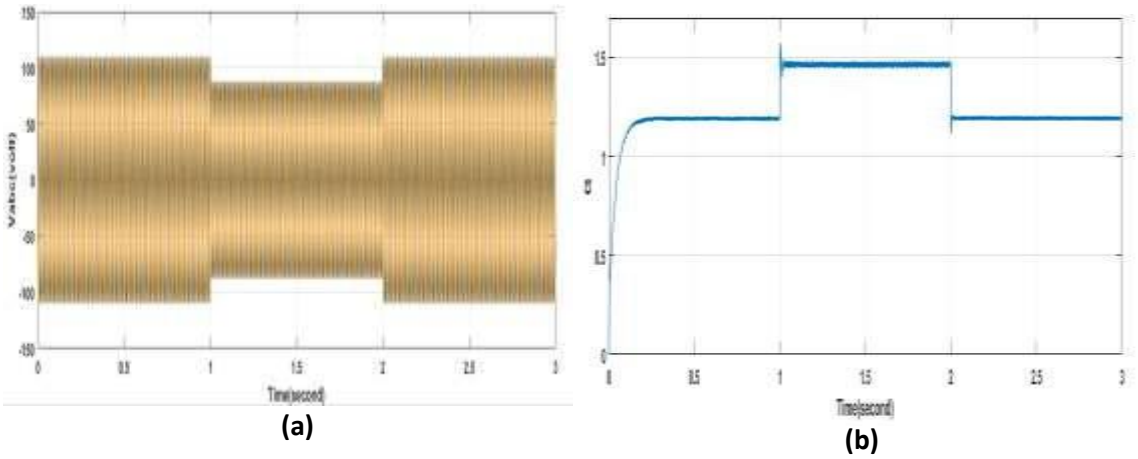

Figure 22 : (a) Three phase input supply voltages of case , (b) Voltage gain response of case 3

as shown in figure (23. a) and m_i= 0.712. It is clear from figure (23. b) that the dc-link voltage boosts higher than its original value during voltage sag according to proposed control strategy of D based on required speed to maintain the motor speed constant at 3000 rpm .

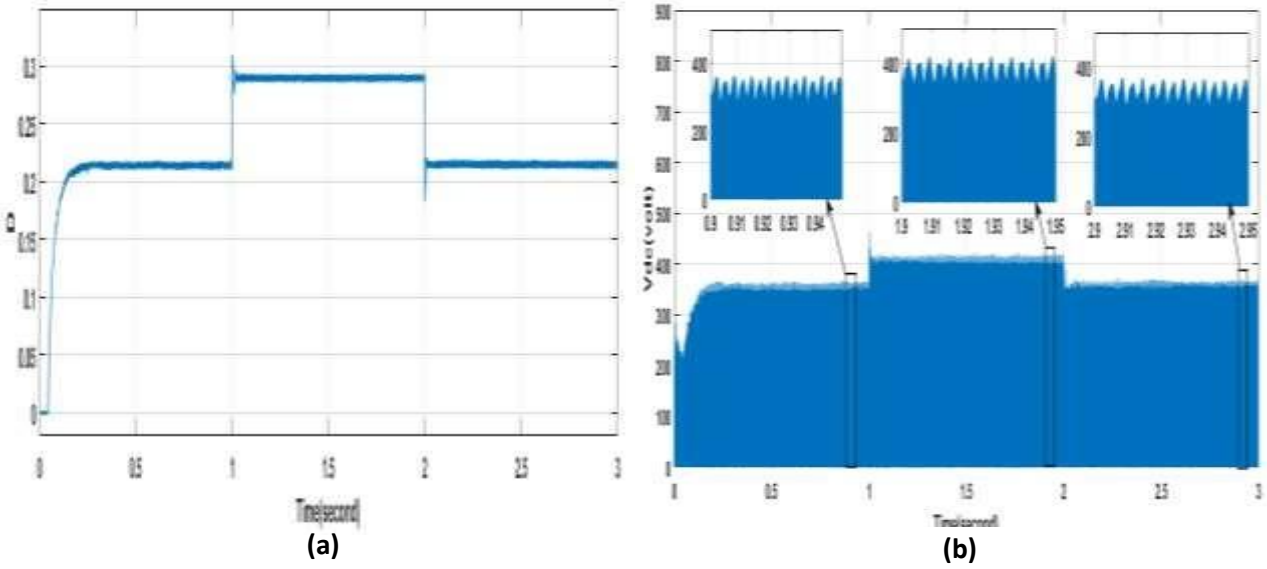

Figure 23 : (a) . D response of case (b) . DC- link voltage of case3

The peak currents through the inductors are 10.5A for both L_1, L_2 ,the peak voltages on capacitors are 173 V and 75 V for both $C_1$and C_2,respectively, also the switch current and voltage are 20.3A and 237 V, respectively of QZSN during voltage sag in case 3. Figure (24.a) shows that the speed response with downshoot of 0.5666% and overshoot of 0.5% at beginning of applied voltage sag, the downshoot and overshoot are 0.3666% and

0.4666%, respectively at removal of voltage sag, and the peak to peak steady state ripple in speed during voltage sag is 0.166%. In Figure (24.b) the torque response is shown.

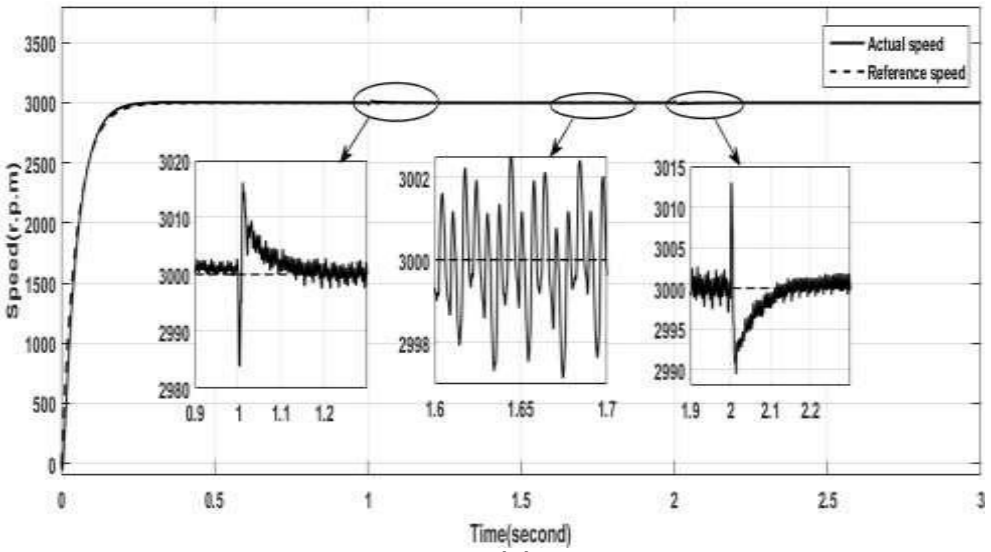

(a)

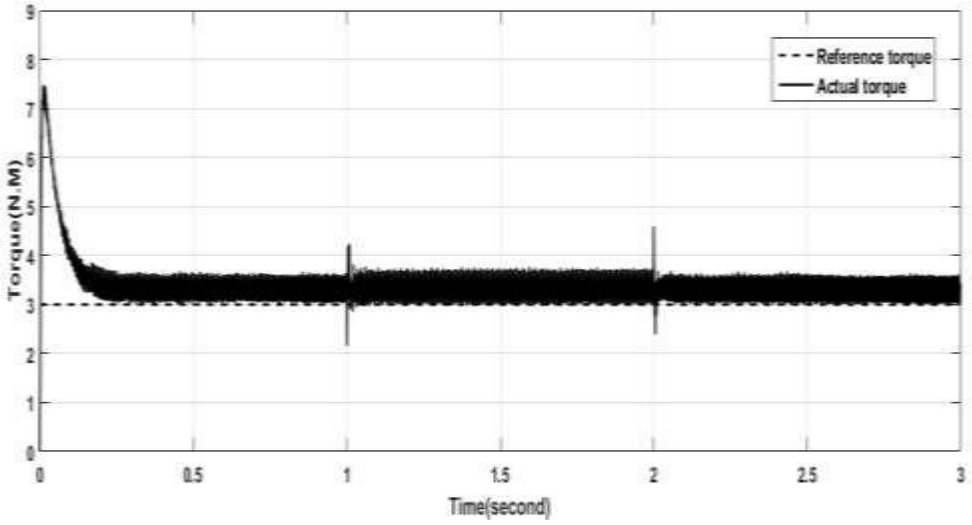

(b)

Figure 24 : (a) The speed response of case 3 , (b) The torque response of case 3

As shown in Figure (25), the amplitude of the source current increases during the voltage drop with a THD of 4.65%, 4.88% and 4.66% before voltage sag, during voltage sag and after voltage sag, respectively.

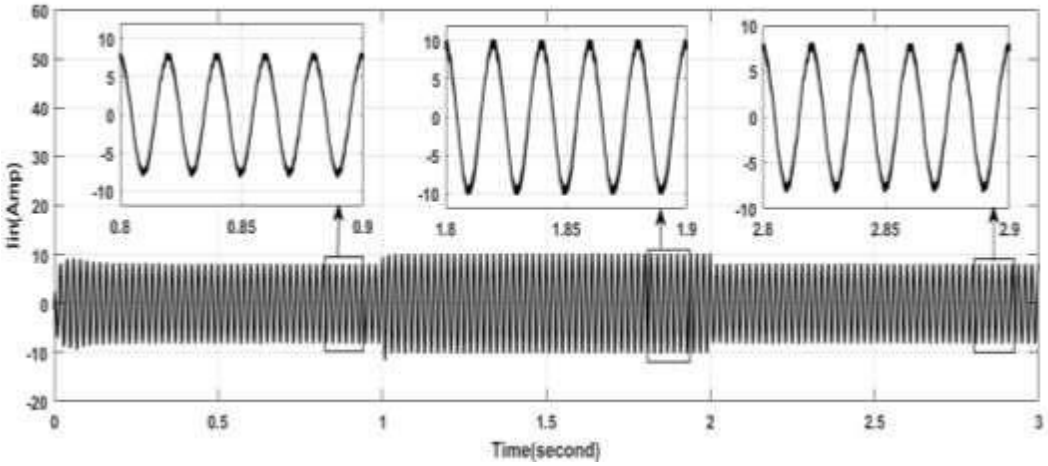

Figure 25 : The phase-a source current waveform of case 3

In Figure (26) it is shown that the stator current waveform has THD of 3.75%, 3.7% and 3.74% before voltage sag, during voltage sag and after voltage sag, respectively.

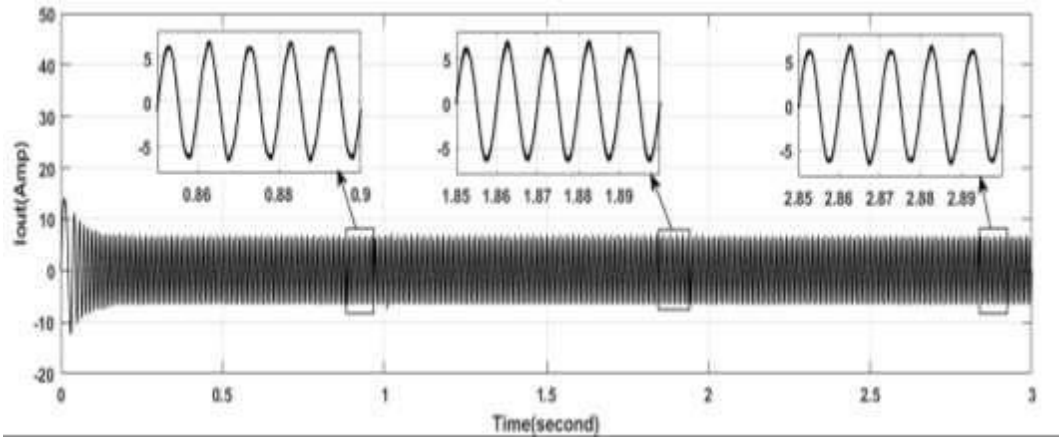

Figure 26 : The phase-A stator current waveform of case 3

10. CONCLUSION:

In this paper , the PMSM is driven by three-phase QZS-IMC, and the following conclusions are outcome:

1. The continuous QZS-IMC has ability to boost the output voltage with boost factor of 3.488 and voltage gain of 1.926 for the D of 0.355 in addition to all advantages of conventional IMC.
2. The QZSN in utilized converter has advantage, that the grid current is in continuous current mode, and THD of the current waveform is less than 7% without using input filter, these features contribute to reduce a size and cost of converter.
3. It is found that voltage and current stresses of inductors, capacitors and IGBT switches in QZSN of utilized converter are increased with increasing shoot-through duty ratio to raise output voltage during voltage sags in three-phase input voltages, this must take in account in design of QZSN.
4. The control strategy of D for the voltage boost is utilized to vary the voltage gain of QZS-IMC during grid voltage sags, speed and load changes, this control strategy is also useful to reduce the current and voltage stresses in QZSN through selection optimal value of D.

REFERENCES

[1] B. BK, "Modern Power Electronics and AC Drives", Englewood Cliffs, NJ: Prentice-Hall, 2002.

[2] D. Sri Vidhya, T. Venkatesan," A Review on Performance Analysis of Matrix Converter Fed AC Motor Drive", International Journal of Power Electronics and Drive System (IJPEDS), Vol. 7, No. 1, pp. 85-93 March 2016.

[3] T. Friedli, J. W. Kolar, J. Rodriguez, and P. W. Wheeler, "Comparative Evaluation of Three-Phase AC–AC Matrix Converter and Voltage DC- Link Back-to-Back Converter Systems", IEEE Transactions on Industrial Electronics, Vol. 59, No. 12, pp. 4487-4510, December 2012.

[4] P. W. Wheeler, J. Rodriguez, J. C. Clare, and L. Empringham, "Matrix converter: A technology review," IEEE Trans. Ind. Electron., vol. 49, no. 2, pp. 276–288, Apr. 2002.

[5] M. Jussila and H. Tuusa "Comparison of Direct and Indirect Matrix Converters in Induction Motor Drive", 32nd Annual Conference on IEEE Industrial Electronics, IECON 2006, pp.1621,1626, 6-10 Nov. 2006.

[6] C. Klumpner, F. Blaabjerg, I. Boldea, and P. Nielsen, "New modulation method for matrix converters," IEEE Transactions on Industry Applications, vol. 42, pp. 797-806, May-Jun 2006.

[7] E. Karaman, M. Farasat and A. M. Trzynadlowski, "A Comparative Study of Series and Cascaded Z-Source Matrix Converters," in IEEE Transactions on Industrial Electronics, vol. 61, no. 10, pp. 5164-5173, Oct. 2014, doi: 10.1109/TIE.2014.2301766.

[8] W. Song, Y. Zhong, H. Zhang, X. Sun, Q. Zhang, W. Wang, "A study of Z-source dual-bridge matrix converter immune to abnormal input voltage disturbance and with high voltage transfer ratio," IEEE Trans. Ind. Informat., vol.9, no.2, pp.828-838, May 2013.

[9] B. Ge, Q. Lei, W. Qian, F. Z. Peng, "A family of Z-source matrixconverters," IEEE Trans. Ind. Electron., vol.59, no.1, pp.35-46, Jan. 2012.

[10] S. Liu, B. Ge, H. Abu-Rub, F. Z. Peng, and Y. Liu, "Quasi-Z-source matrix converter based induction motor drives," in IECON 2012 - 38th Annual Conference on IEEE Industrial Electronics Society, pp.5303- 5307, 25-28 Oct. 2012.

[11] O. Ellabban, H. Abu-Rub, and S. Bayhan, "Z-source matrix converter: an overview," IEEE Trans. Ind. Electron., vol. 31, no. 11, pp. 7436-7450, Aug. 2015.

[12] L. Shuo, G. Baoming, J. Xinjian, H. Abu-Rub and F. Z. Peng, "Comparative Evaluation of Three Z-Source/Quasi-Z-Source Indirect Matrix Converters", IEEE Transactions on Industrial Electronics, vol. 62, no. 2, pp. 692-701, Feb. 2015.

[13] S. Liu1, B. Ge, X. You1, X. Jiang, H. Abu- Rub and F. Z. Peng, "A novel quasi-Z-source indirect matrix converter", The International Journal of Circuit Theory and Applications Int. J. Circ. Theor. Appl. 2015; 43:438–454.

[14] X. You, B. Ge, S. Liu, N. Nie, X. Jiang and H. Abu-Rub, "Common mode voltage reduction of quasi-Z source indirect matrix converter", International Journal of Circuit Theory and Applications, March 2015.

[15] Pragasen Pillay and Ramu Krishnan,"Control Characteristics and SpeedControl Design for a High Performance PMSM Drive", IEEE Transaction on power Electronics, vol .5, no. 2, April,1990.

[16] Z. Mahmood, "Speed Performance Based Vector-Controlled Permeant Magnet Synchronous Motor Fed by Indirect Matrix Converter ", M. Sc. thesis, Department of Electrical Engineering, University of Al- Mustansiriyah,2018.

[17] H. Zhu, X. Xiao and Y. Li, "PI type dynamic decoupling control scheme for PMSM high speed operation," 2010 Twenty-Fifth Annual IEEE Applied Power Electronics Conference and Exposition (APEC), Palm Springs, CA, USA, 2010, pp. 1736-1739, doi: 10.1109/APEC.2010.5433467.